

# 1 **Uncertainty assessment of a dominant-process catchment** 2 **model of dissolved phosphorus transfer**

3 **R. Dupas<sup>1</sup>, J. Salmon-Monviola<sup>1</sup>, K. Beven<sup>2</sup>, P. Durand<sup>1</sup>, P.M. Haygarth<sup>2</sup>, M.J.**  
4 **Hollaway<sup>2</sup>, C. Gascuel-Odoux<sup>1</sup>**

5 [1] INRA, Agrocampus Ouest, UMR1069 SAS, F-35000 Rennes, France

6 [2] Lancaster Environment Centre, Lancaster University, Lancaster, United Kingdom, LA1  
7 4YQ

8 Correspondence to: R. Dupas (remi.dpas@gmail.com)

## 9 **Abstract**

10 We developed a parsimonious topography-based hydrologic model coupled with a soil  
11 biogeochemistry sub-model in order to improve understanding and prediction of Soluble  
12 Reactive Phosphorus (SRP) transfer in agricultural headwater catchments. The model  
13 structure aims to capture the dominant hydrological and biogeochemical processes identified  
14 from multiscale observations in a research catchment (Kervidy-Naizin, 5 km<sup>2</sup>). Groundwater  
15 fluctuations, responsible for the connection of soil SRP production zones to the stream, were  
16 simulated with a fully-distributed hydrologic model at 20 m resolution. The spatial variability  
17 of the soil phosphorus status and the temporal variability of soil moisture and temperature,  
18 which had previously been identified as key controlling factor of SRP solubilisation in soils,  
19 were included as part of an empirical soil biogeochemistry sub-model. The modelling  
20 approach included an analysis of the information contained in the calibration data and  
21 propagation of uncertainty in model predictions using a GLUE “limits of acceptability”  
22 framework. Overall, the model appeared to perform well given the uncertainty in the  
23 observational data, with a Nash-Sutcliffe efficiency on daily SRP loads between 0.1 and 0.8  
24 for acceptable models. The role of hydrological connectivity via groundwater fluctuation, and  
25 the role of increased SRP solubilisation following dry/hot periods were captured well. We  
26 conclude that in the absence of near continuous monitoring, the amount of information  
27 contained in the data is limited hence parsimonious models are more relevant than highly  
28 parameterised models. An analysis of uncertainty in the data is recommended for model  
29 calibration in order to provide reliable predictions.

# 1   **1   Introduction**

2   Excessive phosphorus (P) concentrations in freshwater bodies result in increased  
3   eutrophication risk worldwide (Carpenter et al., 1998; Schindler et al., 2008). Eutrophication  
4   restricts economic use of water and poses a serious hazard to ecosystems and humans  
5   (Serrano et al., 2015). In western countries, reduction of point source P emissions in the last  
6   two decades has resulted in a proportionally increasing contribution of diffuse sources, mainly  
7   from agricultural origin (Alexander et al., 2008; Grizzetti et al., 2012; Dupas et al., 2015a).  
8   Of particular concern are dissolved P forms, often measured as Soluble Reactive Phosphorus  
9   (SRP), because they are highly bioavailable and therefore a likely contributor to  
10   eutrophication.

11   To reduce SRP transfer from agricultural soils it is important to identify the spatial origin of P  
12   sources in agricultural landscapes, the biogeochemical mechanisms causing SRP  
13   solubilisation in soils and the dominant transfer pathways, as well as the potential P resorption  
14   during transit. Research catchments provide useful data to investigate SRP transport  
15   mechanisms: typically, the temporal variations in water quality parameters at the outlet,  
16   together with hydroclimatic variables, are investigated to infer spatial origin and dominant  
17   transfer pathways of SRP (Haygarth et al., 2012; Outram et al., 2014; Dupas et al., 2015b;  
18   Mellander et al., 2015; Perks et al., 2015). Hypotheses drawn from analysis of water quality  
19   time series can be further investigated through hillslope monitoring and/or laboratory  
20   experiments (Heathwaite and Dils, 2000; Siwek et al., 2013; Dupas et al., 2015c). When  
21   dominant processes are considered reasonably known, it is possible to develop computer  
22   models, for two main purposes: first, to validate scientific conceptual models, by testing  
23   whether model predictions can produce reasonable simulations compared to observations. Of  
24   particular interest is the possibility to test the capability of a computer model to upscale P  
25   processes observed at fine spatial resolution (soil column, hillslope) to a whole catchment.  
26   Second, if the models survive such validation tests, then they can be useful tools to simulate  
27   the response of a catchment system to a future perturbation such as changes in agricultural  
28   management and climate changes.

29   However, process-based P models generally perform poorly compared to, for example,  
30   nitrogen models (Wade et al., 2002; Dean et al., 2009; Jackson-Blake et al., 2015a). This is of  
31   major concern because poor model performance suggests poor knowledge of dominant  
32   processes at the catchment scale, and poor reliability of the modelling tools used to support

1 management. The origin of poor model performance might be conceptual misrepresentations,  
2 structural imperfection, calibration problems, irrelevant model evaluation criteria and  
3 difficulties in properly assessing the information content of the available data when it is  
4 subject to epistemic error. All five causes of poor model performance are intertwined, e.g.  
5 model calibration strategy depends on model performance evaluation criteria, which depend  
6 on the way the information contained in the observation data is assessed (Beven and Smith,  
7 2015).

8 A key issue in environmental modelling is the level of complexity one should seek to  
9 incorporate in a model structure. Several existing P transfer models, such as INCA (Wade et  
10 al., 2002), SWAT (Arnold et al., 1998) and HYPE (Lindstrom et al., 2010) seek to simulate  
11 many processes, with the view that complex models are necessary to understand processes  
12 and to predict the likely consequences of land-use or climate changes. However, these  
13 complex models include many parameters that need to be calibrated, while the amount of data  
14 available for calibration is often low. An imbalance between calibration requirement and the  
15 amount of available observation data can lead to equifinality issues, i.e. when many model  
16 structures or parameter sets lead to acceptable simulation results (Beven, 2006). A  
17 consequence of equifinality is the risk of unreliable prediction when an “optimal” set of  
18 parameters is used (Kirchner, 2006), and large uncertainty intervals when Monte Carlo  
19 simulations are performed (Dean et al., 2009). In this situation, it will be worth exploring  
20 parsimonious models that aim to capture the dominant hydrological and biogeochemical  
21 processes controlling SRP transfer in agricultural catchment. For example, Hahn et al. (2013)  
22 used a soil-type based rainfall-runoff model (Lazzarotto et al., 2006) combined with an  
23 empirical model of soil SRP release derived from rainfall simulation experiments over soils  
24 with different P content and manure application level/timing (Hahn et al., 2012) to simulate  
25 daily SRP load from critical sources areas.

26 A second key issue, linked to the question of model complexity, concerns model calibration  
27 and evaluation. Both calibration and evaluation require assessing the fit of model outputs with  
28 observation data. However, observation data are generally not directly comparable with model  
29 outputs, because of incommensurability issues and/or because they contain errors (Beven,  
30 2006; 2009). Typically, predicted daily concentrations and/or loads are evaluated against data  
31 from grab samples collected on a daily or weekly basis. The information content of these data  
32 must be carefully evaluated to propagate uncertainty in the data into model predictions

1 (Krueger et al., 2012). Uncertainty in grab sample data might stem from i) sampling  
2 frequency problems and ii) measurement problems (Lloyd et al., 2015). Grab sample data  
3 represent a snapshot of the concentration at a given time of the day, which can differ from the  
4 flow weighted mean daily concentration (McMillan et al. 2012), and a specific point in the  
5 stream cross-section, which can differ from the cross section mean concentration (Rode and  
6 Suhr, 2007). This difference between observation data and simulation output can be large  
7 during storm events in small agricultural catchments, as P concentrations can vary by several  
8 orders of magnitudes during the same day (Heathwaite and Dils, 2000; Sharpley et al., 2008).  
9 Model evaluation can be severely penalised by this difference, because many popular  
10 evaluation criteria such as the Nash-Sutcliffe efficiency (NSE) are sensitive to extreme values  
11 and errors in timing (Moriassi et al.,2007). During baseflow periods, it is more likely that grab  
12 sample data are comparable to flow-weighted mean daily concentrations, as concentrations  
13 vary little during the day and they are usually low in the absence of point sources. However,  
14 measurement errors are expected to occur at low concentrations, either due to too long storage  
15 times or laboratory imprecision when concentrations come close to detection/quantification  
16 limits (Jarvie et al., 2002; Moore and Locke, 2013). Uncertainty in the data can also relate to  
17 discharge measurement and input data (e.g. maps of soil P content and rainfall data). In this  
18 paper we strive to identify and quantify the different sources of uncertainty in the data when  
19 the required quality check tests have been performed. A Generalised Likelihood Uncertainty  
20 Estimation (GLUE) “limits of acceptability” approach (Beven, 2006; Beven and Smith, 2015)  
21 is used to calibrate/evaluate the model.

22 This paper presents a dominant-process model that couples a topography-based hydrologic  
23 model with a soil biogeochemistry sub-model able to simulate daily discharge and SRP loads.  
24 The dominant processes included in the hydrologic and soil biogeochemistry sub-models have  
25 been identified in previous analyses of multiscale observational data, which have  
26 demonstrated on the one hand the control of groundwater fluctuation on connecting soil SRP  
27 production zones to the stream (Haygarth et al., 2012; Jordan et al., 2012; Dupas et al., 2015b;  
28 2015d; Mellander et al., 2015), and on the other hand the role of antecedent soil moisture and  
29 temperature conditions on SRP solubilisation in soils (Turner and Haygarth, 2001; Blackwell  
30 et al., 2009; Dupas et al., 2015c). Model development and application was performed in the  
31 Kervidy-Naizin catchment in western France with the objectives of: i) testing if the model  
32 was capable of capturing daily variation of SRP load, thus confirming hypotheses on  
33 dominant processes; ii) develop a methodology to analyse and propagate uncertainty in the

1 data into model prediction using a “limits of acceptability” approach. Model development and  
2 analysis of uncertainty in the data are interlinked in this approach.

## 3 **2 Material and methods**

### 4 **2.1 Study catchment**

#### 5 **2.1.1 Site description**

6 Kervidy–Naizin is a small (4.94 km<sup>2</sup>) agricultural catchment located in central Brittany,  
7 Western France (48°N, 3°W). It belongs to the AgrHyS environmental research observatory  
8 ([http://www6.inra.fr/ore\\_agrhys\\_eng](http://www6.inra.fr/ore_agrhys_eng)), which studies the impact of agricultural activities and  
9 climate change on water quality (Molenat et al., 2008; Aubert et al., 2013; Salmon-Monviola  
10 et al., 2013; Humbert et al., 2014). The catchment (Fig. 1) is drained by a stream of second  
11 Strahler order, which generally dries up in August and September. The climate is temperate  
12 oceanic, with mean  $\pm$  standard deviations of annual cumulative precipitation and specific  
13 discharge of  $854 \pm 179$  mm and  $290 \pm 106$  mm, respectively, from 2000 to 2014. Mean  
14 annual  $\pm$  standard deviation of temperature is  $11.2 \pm 0.6^\circ\text{C}$ . Elevation ranges from 93 to 135  
15 m above sea level. Topography is gentle, with maximum slopes not exceeding 5%. The  
16 bedrock consists of impervious, locally fractured Brioverian schists and is capped by several  
17 metres of unconsolidated weathered material and silty, loamy soils. The hydrological  
18 behaviour is dominated by the development of a water table that varies seasonally along the  
19 hillslope. In the upland domain, consisting of well drained soils, the water table remains  
20 below the soil surface throughout the year, varying in depth from 1 to > 8 m. In the wetland  
21 domain, developed near the stream and consisting of hydromorphic soils, the water table is  
22 shallower, remaining near the soil surface generally from October to April each year. The  
23 land use is mostly agriculture, specifically arable crops and confined animal production (dairy  
24 cows and pigs). A farm survey conducted in 2013 led to the following land use subdivisions:  
25 35% cereal crops, 36% maize, 16% grassland and 13% other crops (rape seed, vegetables).  
26 Animal density was estimated as high as 13 livestock units ha<sup>-1</sup> in 2010. Estimated soil P  
27 surplus was 13.1 kg P ha<sup>-1</sup> yr<sup>-1</sup> (Dupas et al., 2015b) and soil extractable P in 2013 (Olsen et  
28 al., 1954) was  $59 \pm 31$  mg P kg<sup>-1</sup> (n = 89 samples). A survey targeting riparian areas  
29 highlighted the legacy of high soil P content in these currently unfertilized areas (Dupas et al.,  
30 2015c). No point source emissions were recorded but scattered dwellings with septic tanks  
31 were present in the catchment.

## 1 **2.1.2 Hydroclimatic and chemical monitoring**

2 Kervidy-Naizin was equipped with a weather station (Cimel Enerco 516i) located 1.1 km  
3 from the catchment outlet. It recorded hourly precipitation, air and soil temperatures, air  
4 humidity, global radiation, wind direction and speed, and estimates Penman  
5 evapotranspiration. Stream discharge was estimated at the outlet with a rating curve and stage  
6 measurements from a float-operator sensor (Thalimèdes OTT) upstream of a rectangular weir.  
7 To record both seasonal and within storm dynamics in P concentration, two monitoring  
8 strategies complemented each other from October 2013 to August 2015: a daily manual grab  
9 sampling at approximately the same time (between 16:00 – 18:00 local time) and automatic  
10 high frequency sampling during 14 storm events (autosampler ISCO 6712 Full-Size Portable  
11 Sampler, 24 one litre bottles filled every 30 min). The water samples were filtered on-site,  
12 immediately after grab sampling and after 1-2 days in the case of autosampling. They were  
13 analysed for SRP (ISO 15681) within a fortnight. To assess uncertainty in daily SRP  
14 concentration related to sampling time, storage and measurement errors, a second grab sample  
15 was taken at a different time of the day (between 11:00 – 15:00 local time) in 36 instances  
16 during the study period. The second sample was analysed within 24h with the same method;  
17 this second dataset is referred to as verification dataset, as opposed to the reference dataset.  
18 Among the 36 pairs of comparable daily samples, 12 were taken during storm events and 24  
19 during baseflow periods. To assess uncertainty in high frequency SRP concentration during  
20 storm events due to delayed filtration of autosampler bottles, 5 grab samples were taken  
21 during the course of 4 distinct storms and were filtered immediately. The same lab procedure  
22 was used to analyse SRP.

## 23 **2.1.3 Identification of dominant processes from multiscale observations**

24 Observations in the Kervidy-Naizin catchment have highlighted that the temporal variability  
25 in stream SRP concentrations could not be related to the calendar of agricultural practices, but  
26 rather to hydrological and biogeochemical processes (Dupas et al., 2015b). The primary  
27 control of hydrology on SRP transfer has also been evidenced in several other small  
28 agricultural catchments (e.g. Haygarth et al, 2012; Jordan et al., 2012; Mellander et al., 2015).  
29 In the Kervidy-Naizin catchment, groundwater fluctuations in valley bottom areas was  
30 identified as the main driving factor of SRP transfer, through the hydrological connectivity it  
31 creates when it intercepts shallow soil layers (Dupas et al., 2015b).

1 In-situ monitoring of soil pore water at 4 sites (15 cm and 50 cm depths) in the Kervidy-  
2 Naizin catchment has shown that mean SRP concentration in soils was a linear function of  
3 Olsen P (Olsen et al., 1954). This reflects current knowledge that a soil P test, or alternatively  
4 estimation of a degree of P saturation, can be used to assess solubilisation in soils  
5 (Beauchemin and Simard, 1999; McDowell et al., 2002; Schoumans et al., 2015). This linear  
6 relationship derived from the data contrasts however with other studies, where threshold  
7 values above which SRP solubilisation increases greatly have been identified (Heckrath et al.,  
8 1995; Maguire et al., 2002).

9 Soluble Reactive Phosphorus solubilisation in soil varies seasonally according to antecedent  
10 conditions of temperature and soil moisture. Dry and/or hot conditions are favourable to  
11 accumulation of mobile P forms in soils, while water saturated conditions lead to their  
12 flushing (Turner et al., 2001; Blackwell et al., 2009; Dupas et al., 2015c).

## 13 **2.2 Description of the Topography-based Nutrient Transfer and** 14 **Transformation – Phosphorus model (TNT2-P)**

15 TNT2 was originally developed as a process-based and spatially explicit model simulating  
16 water and nitrogen fluxes at a daily time step (Beaujouan et al., 2002) in meso-scale  
17 catchments ( $< 50 \text{ km}^2$ ). TNT2-N has been widely used for operational objectives, to test the  
18 effect of mitigation options proposed by local stakeholders or public policy-makers (Moreau  
19 et al., 2012; Durand et al., 2015), on nitrate fluxes and concentrations in rivers.

20 TNT2-P uses a modified version of the hydrological sub-model in TNT2-N, to which a P  
21 biogeochemistry sub-model was added to simulate SRP solubilisation in soils.

### 22 **2.2.1 Hydrological sub-model**

23 The assumptions in the hydrological sub-model are derived from TOPMODEL which has  
24 previously been applied to the Naizin catchment (Bruneau et al., 1995; Franks et al., 1998): 1)  
25 the effective hydraulic gradient of the saturated zone is approximated by the local topographic  
26 surface gradient ( $\tan \beta$ ). It is calculated in each cell of a Digital Elevation Model (DEM) at the  
27 beginning of the simulation; 2) the effective downslope transmissivity (parameter T) of the  
28 soil profile in each cell of the DEM is a function of the soil moisture deficit (Sd). Hydraulic  
29 conductivity decreases exponentially with depth (parameter m, Fig. 2). Hence water fluxes (q)  
30 are computed as:

$$1 \quad q = T * \tan\beta * \exp\left(-\frac{Sd}{m}\right) \quad (1)$$

2 Based on these assumptions, TNT2 computes an explicit cell-to-cell routing of fluxes, using a  
3 D8 algorithm.

4 To simulate SRP fluxes, the only modification to the hydrological sub-model aimed to  
5 compute water fluxes from each soil layer by integrating [1] between the maximum depth of  
6 the soil layer considered and:

7 - estimated groundwater level, if the groundwater table is within the soil layer  
8 considered

9 or

10 - the minimum depth of the soil layer considered, if the groundwater table above the  
11 soil layer considered

12 In this application of the TNT2-P model, 5 soil layers with a thickness of 10 cm are  
13 considered. Hence, 7 flow components are computed in the model:

- 14 - overland flow on saturated surface
- 15 - 5 sub-surface flow components, for each soil layer
- 16 - deep flow, i.e. flow below the 5 soil layers

### 17 **2.2.2 Soil-P sub-model**

18 The soil-P sub-model is empirically derived from soil pore water monitoring data (Dupas et  
19 al., 2015c), specifically assuming that:

- 20 - background SRP concentration in the soil pore water of a given layer is proportional to  
21 soil Olsen P;
- 22 - seasonal increases in P availability compared to background conditions are determined  
23 by biogeochemical processes, controlled by antecedent temperature and soil moisture.  
24 Data show that SRP availability in the soil pore water increases following periods of  
25 dry and hot conditions (Dupas et al., 2015c).

26 Hence, SRP transfer is modelled with parameters that describe both mobilisation and transfer  
27 to the stream. A different parameter is used to simulate transfer via overland flow and sub-  
28 surface flow.

$$29 \quad F_{SRP \text{ overland}} = Coef_{SRP \text{ overland}} * P_{Olsen} * q_{overland} \quad (2)$$



$$1 \quad F_{SRP \text{ sub-surface}} = Coef_{SRP \text{ sub-surface}} * P_{Olsen} * q_{\text{sub-surface}} \quad (3)$$

2 Where  $F_{SRP \text{ overland}}$  and  $F_{SRP \text{ sub-surface}}$  are SRP transfer via overland flow and sub-surface  
 3 flow for a given soil layer respectively,  $q_{\text{overland}}$  and  $q_{\text{sub-surface}}$  are water flows from the  
 4 same pathways.  $Coef_{SRP \text{ overland}}$  and  $Coef_{SRP \text{ sub-surface}}$  are coefficients which vary  
 5 according to antecedent temperature and soil moisture conditions, such as:

$$6 \quad Coef_{SRP} = Coef_{\text{background}} * (1 + F_T * F_S) \quad (4)$$

7 Where  $Coef_{SRP}$  is either  $Coef_{SRP \text{ overland}}$  or  $Coef_{SRP \text{ sub-surface}}$ , and  $F_T$  and  $F_S$  are  
 8 temperature and soil moisture factors, respectively.  $F_T$  and  $F_S$  are expressed as:

$$9 \quad F_T = \exp\left(\frac{\text{mean}(\text{temperature}, i \text{ days}) - T_1}{T_2}\right) \quad (5)$$

$$10 \quad F_S = 1 - \left(\frac{\text{mean}(\text{water content}, i \text{ days})}{\text{maximum water content}}\right)^{S1} \quad (6)$$

11 Where  $T_1$ ,  $T_2$  and  $S1$  are calibrated coefficients. The antecedent condition time length  
 12 consists in a period of  $i=100$  days. Both soil temperature and soil moisture are estimated by  
 13 TNT2 soil module (Moreau et al., 2013). Because soil moisture in the deep soil layers can  
 14 differ significantly from that of shallow soil layers, two values of  $F_S$  are calculated for two  
 15 soil depth 0-20 cm and 20-50 cm. The temperature factor  $F_T$  was calculated as an average  
 16 value for the entire soil profile 0-50 cm. Contrary to water fluxes, SRP fluxes are not routed  
 17 cell-to-cell, because we lacked knowledge of the rate of SRP re-adsorption in downslope  
 18 cells, and on the long term fate of re-adsorbed SRP. Hence, all the SRP emitted from each cell  
 19 through overland flow and sub-surface flow reaches the stream on the same day. For deep  
 20 flow, only the immediate riparian flux is used in determining SRP inputs to the river.

21 No long-term depletion of the different P pools was modelled, because P export from the  
 22 catchment was small compared to the size of soil and sub-soil P pools.

### 23 **2.2.3 Input data and parameters**

24 Spatial input data include:

- 25 - A DEM in raster format. Here, a 20 m resolution DEM was used, hence model  
 26 calculations were made in 12348 grid cells covering a 4.94 km<sup>2</sup> catchment.
- 27 - A map of soils with homogeneous hydrological parameter value, in raster format.  
 28 Here, two soil classes were considered by differentiating well-drained (86%) and  
 29 poorly drained soils (14%) according to Curmi et al. (1998) (Fig. 1).

1 - A map of surface Olsen P in raster format and description of decrease in P Olsen with  
2 depth for five soil layers between 0-50 cm. Here, the map of Olsen P in the 0-15 cm  
3 soil layer was obtained from statistical modelling with the rule-based regression  
4 algorithm CUBIST (Quinlan, 1992) using data from 198 soil samples (2013) in an  
5 area of 12 km<sup>2</sup> encompassing the 4.94 km<sup>2</sup> catchment (Matos-Moreira et al., 2015).  
6 To describe how P Olsen decreases with depth, land use information was used. In  
7 tilled fields, i.e. all crop rotations including arable crops, Olsen P was assumed to be  
8 constant between 0-30 cm and to decrease linearly with depth between 30-50 cm. In  
9 no-till fields, i.e. permanent pasture and woodland, Olsen P was assumed to decrease  
10 linearly with depth between 0-50 cm. An exponential decrease with depth is more  
11 commonly adopted in untilled land (e.g. Haygarth et al., 1998; Page et al., 2005), but a  
12 specific sampling in currently untilled areas in the Kervidy-Naizin catchment (Dupas  
13 et al., 2015c) has shown that a linear function is more appropriate, probably because  
14 of these areas having been ploughed in the past.

15 Climate input data include minimum and maximum air temperature, precipitation, potential  
16 evapotranspiration, global radiation on a daily basis. The TNT2 model allows for several  
17 climate zones to be considered, in which case a raster map of climate zone must be provided  
18 to the model. Here, only one climate zone is considered.

19 In total, the TNT2-P model includes 15 parameters for each soil type, i.e. 30 parameters in  
20 total if two soil drainage classes are considered. To reduce the number of model runs  
21 necessary to explore the parameter space using Monte Carlo simulations, several parameters  
22 were given fixed values, or a constant ratio between the two soil types was set (Table 1). In  
23 the hydrological sub-model, the parameters to vary were identified in a previous sensitivity  
24 analysis (Moreau et al., 2013). In the soil sub-model, all the parameters were varied.

25 Finally, only 12 parameters were varied independently. Initial parameter ranges for the  
26 hydrological sub-model were based on values from several previous studies in Western  
27 France (Moreau et al., 2013) and those for the soil sub-model were based on a preliminary  
28 manual trial and error procedure. The SRP concentration for deep flow water was based on  
29 actual measurement of SRP in the weathered schist (Dupas et al., 2015c). A constant flux  
30 value for domestic sources was set at the 1% percentile of the daily flux between 2007 and  
31 2013 (Dupas et al., 2015b).

## 1 **2.3 Deriving limits of acceptability from data uncertainty assessment**

2 The Monte Carlo based Generalized Likelihood Uncertainty Estimation (GLUE)  
3 methodology has been widely used in hydrology and is described elsewhere (Beven and  
4 Freer, 2001a; Beven, 2006, 2009). Briefly, the rationale of GLUE is that many model  
5 structures and parameter sets can give “acceptable” results, according to one or several  
6 performance measures, due to equifinality. Hence, GLUE considers that all models that give  
7 acceptable results should be used for prediction. A key issue in GLUE is to decide on a  
8 performance threshold to define acceptable models; typically, modellers set a threshold value  
9 of a measure such as the Nash-Sutcliffe Efficiency based on their subjective appreciation of  
10 data uncertainty or on previously used values. To allow for a more explicit justification of the  
11 performance threshold values used, the limits of acceptability approach outlined by Beven  
12 (2006) relies on an assessment of uncertainty in the calibration/evaluation data. According to  
13 this approach, all model realisations that fall within the limits of acceptability are used for  
14 prediction, weighted by a score calculated based on overall performance.

15 Details on how the limits of acceptability for daily discharge and daily SRP load were derived  
16 from uncertainty assessment of the observational data are presented below. Input data, such as  
17 weather and soil Olsen P data, also contained uncertainty which were not accounted for  
18 explicitly in the limits of acceptability due to a lack of data to quantifying them.

### 19 **2.3.1 Discharge**

20 Error in discharge measurement data was assessed from the original discharge measurements  
21 used to calibrate the stage-discharge rating curve (Carluer, 1998). The rating curve used in  
22 this study was:

$$23 \quad Q = a * (h - h_0)^b \quad (7)$$

24 Where Q is discharge, h is stage reading,  $h_0$  is stage reading at zero discharge, a and b are  
25 calibrated coefficients. Limits of acceptability were defined as the 90% prediction interval of  
26 log-log linear regression (Fig. 3). The acceptability range estimated in this way was  $\pm 39\%$  on  
27 average. This uncertainty interval is in the higher range of values found in other studies, e.g.  
28 Coxon et al. (2015) who found that mean discharge uncertainty was generally between 20%  
29 and 40% in 500 catchments of the United Kingdom. This relatively large uncertainty interval  
30 is due to the fact that it was derived from a prediction interval rather than a confidence  
31 interval (the 90% confidence interval of the log-log linear regression would be 14% of the

1 mean discharge value during the study period). This choice of a relatively large acceptability  
2 interval counterbalances the fact that other sources of uncertainty (e.g. uncertainty in rainfall)  
3 were not accounted for in the discharge limits of acceptability. Moreover, the high percentage  
4 often represents a low absolute value because daily discharge was below  $2 \text{ mm d}^{-1}$  during  
5 78% of the time during the study period. For daily discharge values below  $2 \text{ mm d}^{-1}$ , fixed  
6 acceptability limits were set at the 90% prediction interval for a stage measurement  
7 corresponding to  $2 \text{ mm d}^{-1}$ .

### 8 **2.3.2 SRP load**

9 Uncertainty in “observed” daily load includes uncertainty in discharge (see 2.3.1.) and  
10 uncertainty in SRP concentration. Uncertainty in daily load was estimated summing up  
11 relative uncertainty assessed for discharge and SRP concentration. Uncertainty in SRP  
12 concentration stems from sampling frequency problems as one grab sample collected on a  
13 specific day is incommensurable with the mean daily concentration or load simulated by the  
14 model. Further, measurement errors exist that include the effect of storage time (Haygarth et  
15 al., 1995). During baseflow periods, measurement error was expected to be the main source of  
16 uncertainty because relative measurement error is large for low concentrations, especially  
17 when sample storage time exceeds 48h (Jarvie et al., 2002), while concentrations vary little.  
18 During storm events, sampling frequency was expected to be the main source of uncertainty  
19 because SRP concentration can vary by one order of magnitude within a few hours.  
20 Therefore, different acceptability limits were set for both flow conditions. We considered  
21 storms as events with  $> 20 \text{ l s}^{-1}$  increase in discharge and the following 24h.

22 During baseflow periods, the acceptability limits were derived from the 90% prediction  
23 interval of a linear regression model ( $y = a * x + b$ ) linking pairs of data points sampled on the  
24 same day (reference sample between 16:00-18:00, verification sample between 11:00-15:00)  
25 and analysed independently (within a fortnight for the reference sample and within 1-2 days  
26 for the verification sample). It was assumed that there was no systematic bias between the two  
27 datasets due to different sampling time. The reference SRP concentrations were on average  
28 13% lower than the verification value but this difference was not statistically significant  
29 (Mann-Whitney Rank Sum Test,  $p > 0.05$ ). Hence, the expected underestimation of SRP  
30 concentration due to long sample storage appears to be overshadowed by other sources of  
31 uncertainty such as variability in SRP concentration during the day of sampling or analytical  
32 imprecision at low concentrations. This method encompasses all various sources of

1 uncertainty, which results in prediction intervals much wider than what would result from a  
2 mere repeatability test: at the median concentration ( $0.02 \text{ mg l}^{-1}$ ), estimated prediction interval  
3 was 166% with this method versus 57% with a repeatability test (Fig. 4). As for discharge  
4 estimates, the high percentage represents a small absolute value ( $0.03 \text{ mg l}^{-1}$ ) during baseflow  
5 periods.

6 During storm events, acceptability limits were derived from the 90% prediction interval of  
7 concentration discharge empirical models  $C = a \cdot Q^b$  using high frequency autosampler data.  
8 An empirical model was used to fit to each storm event monitored separately and a delay term  
9 was introduced manually in the empirical model when a time lag existed between  
10 concentration and discharge peaks. The empirical models were then applied to extrapolate  
11 concentration estimation during two days at 10 min resolution, for each of the 14 storm events  
12 monitored. Finally the 2-day mean “observed” load was estimated as the mean of 10 min  
13 loads and uncertainty limits were derived from the 90% prediction interval. In model  
14 evaluation, the mean of simulated loads during 2 consecutive days was evaluated against the  
15 2-day mean “observed” load for which prediction intervals have been calculated. A 2-day  
16 acceptability limit enables all the storm events to be covered (Fig. 5 and Supplement). A 2-  
17 day aggregation was necessary here because increased SRP load as a response to each storm  
18 event could occur either mainly during the day of the rainfall (if the rainfall occurred early in  
19 the morning) or mainly during the day following the rainfall (if the rainfall occurred late in  
20 the evening), and with the daily resolution of the input data and model simulation, the  
21 information about the timing of the rainfall event was not available to the model.

22 When comparing autosampler data with data from immediately filtered samples, the ratio  
23 obtained had the range 1-1.6 (mean = 1.3), hence autosampler data were underestimates of the  
24 true concentration, arguably through adsorption or biological consumption. We used the mean  
25 ratio to correct all storm uncertainty intervals by 30% and the range values to extend the  
26 upper limit by 60%. During days with a storm event not monitored at high frequency with an  
27 autosampler, we considered that the grab sample data did not contain enough information to  
28 derive an acceptability interval for daily SRP load; hence simulated load was not evaluated  
29 for events not monitored at high frequency.

### 30 **2.3.3 Model runs and selection of acceptable models**

31 To explore the parameter space, 20,000 Monte Carlo realisations were performed to simulate  
32 daily discharge and SRP load during the water years 2013-2014 and 2014-2015. The number

1 of Monte Carlo realisations was constrained by the computation time required to run a  
2 spatially explicit model in this catchment but similarity of results were found over both  
3 15,000 and 20,000 runs. A 7-month initialisation period was run to reduce the impact of initial  
4 conditions on simulated results during the study period, from 1 October 2013 to 31 July 2015.

5 To be considered acceptable, model runs must fall within the acceptability limits defined in  
6 2.3.1 and 2.3.2. More specifically, 100% of simulated daily discharge, 100% of simulated  
7 baseflow SRP load and 100% of simulated storm SRP load had to fall within the acceptability  
8 limits. Thus, 572 acceptability tests were performed for discharge, 378 for baseflow SRP load  
9 and 14 for storm SRP loads, i.e. 964 evaluation criteria.

10 To evaluate the model performance in more detail, normalized scores were calculated during  
11 6 periods (Table 2). To calculate the scores, a difference was calculated between each of the  
12 daily simulated discharge, baseflow SRP load and 2-day storm SRP loads and the  
13 corresponding observation. This difference was then normalized by the width of the  
14 acceptability limit defined for that day, so the score has a value of 0 in the case of a perfect  
15 match with observation, -1 at the lower limit and +1 at the upper limit (Fig. 6a). Finally, the  
16 median of this ratio was calculated for each of the 6 periods to investigate whether the model  
17 tended to underestimate or overestimate discharge and loads at different moments of the year  
18 and between the two years.

19 Model runs were successively evaluated for discharge, baseflow SRP load and storm SRP  
20 load. To use the models for prediction, each accepted model was given a likelihood weight  
21 according to how well it has performed for each of the 964 evaluation criteria. Here the  
22 statistical deviation weight was used (truncated to 90% prediction interval) (Fig. 5b).  
23 Calculated weights were then averaged for discharge, baseflow SRP load and storm SRP load  
24 respectively and the final likelihood was calculated as the product of all three averages.

25 The model's sensitivity to each hydrological and soil parameter was performed with a  
26 Hornberger-Spear-Young Generalised Sensitivity Analysis (HSY GSA, Whitehead and  
27 Young, 1979; Hornberger and Spear, 1981). For each evaluation criteria (daily discharge,  
28 daily baseflow SRP load, 2-day storm SRP load), the model runs were split into acceptable  
29 and non-acceptable runs according to the above-mentioned acceptability limits. Then a  
30 Kolmogorov-Smirnov test is performed to assess whether the distribution of each of the three  
31 evaluation criteria differ between acceptable and non-acceptable models for each parameter.  
32 Because the Kolmogorov-Smirnov test might suggest that small differences in distribution are

1 very significant when there are larger number of runs, this method is a qualitative guide to  
2 relative sensitivity. The p value of the Kolmogorov-Smirnov test is used to discriminate  
3 whether the model is critically sensitive ( $p < 0.01$  ‘\*\*\*’), importantly sensitive ( $p < 0.1$  ‘\*’) or  
4 insignificantly sensitive ( $p > 0.1$  ‘.’) to each parameter and for each of the three evaluation  
5 criteria.

6 In addition to acceptability limit approach, a NSE (Moriassi et al., 2007) was calculated for  
7 daily discharge and daily load and concentration to allow comparison with other modelling  
8 studies where it has been taken as an evaluation criteria.

### 9 **3 Results**

#### 10 **3.1 Presentation of observation data and calculation of acceptability limits**

11 The two water years studied were highly contrasted in terms of hydrology and SRP loads.  
12 Water year 2013-2014 was the wettest in the last 10 years, with cumulative rainfall 1289 mm  
13 and cumulative runoff 716 mm. Water year 2014-2015 was an average year (5<sup>th</sup> wettest in the  
14 last 10 years), with cumulative rainfall 677 mm and cumulative runoff 383 mm. Annual SRP  
15 load was  $0.35 \text{ kg P ha}^{-1} \text{ yr}^{-1}$  in 2013-2014 and  $0.17 \text{ kg P ha}^{-1} \text{ yr}^{-1}$  in 2014-2015, i.e. a  
16 difference 10% higher than that of discharge. Observed mean SRP concentration during the  
17 study period was  $0.024 \text{ mg l}^{-1}$ .

18 Fig. 7 a and b show acceptability limits for daily discharge and daily SRP loads. Note that  
19 acceptability limits for discharge were calculated every day, while acceptability limits for  
20 SRP load was calculated on a daily basis during baseflow periods and on a 2-day basis during  
21 storm events monitored at high frequency. No SRP load acceptability limit was calculated  
22 during storm events when no high frequency autosampler data was available.

#### 23 **3.2 Model evaluation**

24 First, model runs were evaluated against acceptability limits defined for discharge (Fig. 7c).  
25 5,479/20,000 models fulfilled the selection criterion for discharge, i.e. they had 100% of  
26 simulated daily discharge within the acceptability limits. The NSE estimated for these models  
27 ranged from 0.75 to 0.93. The normalized scores calculated seasonally (Fig. 8a) show that  
28 simulated discharge is often overestimated in autumn and spring, and underestimated in  
29 winter.

1 Then, model runs were evaluated against acceptability limits defined for SRP loads (Fig. 7d ).  
2 During baseflow periods, 4,964/20,000 models fulfilled the selection criterion for SRP loads,  
3 i.e. they had 100% of simulated daily SRP load within the acceptability limits. Among them,  
4 1,595 also fulfilled the previous selection criterion for discharge. Normalized scores for  
5 baseflow SRP load showed the same trend as for discharge (Fig. 8b), i.e. overestimation in  
6 autumn and spring, and underestimation in winter. During storm events, only 7 models  
7 fulfilled the selection criterion for SRP loads, i.e. they had 14/14 of simulated 2-day storm  
8 SRP loads within the acceptability limits, but none of them also fulfilled the selection criteria  
9 for discharge and baseflow SRP loads. Two storm events were particularly difficult to  
10 simulate (number 2 and number 9, Fig. 8c), probably because their acceptability interval was  
11 very narrow as a result of only small changes in discharge and concentration. To obtain a  
12 reasonable number of acceptable models, we relaxed the selection criterion so that the  
13 acceptable models had to simulate 12/14 of storm loads within the acceptability limits, in  
14 addition to the selection criteria defined for discharge and baseflow SRP load: 539 models  
15 were then accepted. Estimated NSE of these 539 models ranged from 0.09 to 0.81 for daily  
16 load and from negative values to 0.53 for daily concentrations (this includes all data from the  
17 regular sampling).

### 18 **3.3 Sensitivity analysis and prediction results**

19 According to the HSA generalised sensitivity analysis, simulated discharge was critically  
20 sensitive to 10 out of the 12 hydrological parameters varied. Simulated SRP load was  
21 critically sensitive to the sub-surface and overland flow parameters during baseflow periods  
22 and to the overland flow parameter during storm events. During baseflow periods, SRP load  
23 was insignificantly sensitive to the parameter associated with deep flow load. Both baseflow  
24 and storm SRP loads were critically sensitive to the parameter related to soil moisture and soil  
25 temperature dependent SRP solubilisation (S1, T1 and T2), in addition to respectively 12 and  
26 8 hydrological parameters. This identification of sensitive parameters can be used in future  
27 application of the TNT2-P model in the study catchment, as suggested by Whitehead and  
28 Hornberger (1984) and Wade et al. (2002b).

29 Figure 9 shows the daily discharge, SRP load and concentration as simulated by the  
30 acceptable models. Simulated SRP load during the water year 2013-2014 ranged 0.81 – 3.25  
31 kg P ha<sup>-1</sup> yr<sup>-1</sup> (median = 1.68 kg P ha<sup>-1</sup> yr<sup>-1</sup>); simulated SRP load during the water year 2014-  
32 2015 ranged 0.14 – 0.73 kg P ha<sup>-1</sup> yr<sup>-1</sup> (median = 0.34 kg P ha<sup>-1</sup> yr<sup>-1</sup>). Best estimate of SRP



1 load according to observation data was  $0.35 \text{ kg P ha}^{-1} \text{ yr}^{-1}$  in 2013-2014 and  $0.17 \text{ kg P ha}^{-1} \text{ yr}^{-1}$   
2 in 2014-2015. According to the model, 49 – 55% (median = 52%) of water discharge and 66 –  
3 70% (median = 67%) of SRP load occurred during storm events. Mean SRP concentrations  
4 during the two water years ranged  $0.014 – 0.044 \text{ mg l}^{-1}$  (median =  $0.029 \text{ mg l}^{-1}$ ), while mean  
5 observed SRP concentration was  $0.024 \text{ mg l}^{-1}$ .

## 6 **4 Discussion**

### 7 **4.1 Role of hydrology and biogeochemistry in determining SRP transfer**

8 The fairly good performance of TNT2-P at simulating SRP loads provides further support that  
9 the hydrological and biogeochemical processes included into the model are dominant  
10 controlling factors in the Kervidy-Naizin catchment (i.e. the modelling hypotheses could not  
11 be rejected based on this study). The primary control of hydrology in controlling connectivity  
12 between soils and streams has been highlighted by many studies analysing water quality time  
13 series at the outlet of agricultural catchments (Haygarth et al., 2012; Jordan et al., 2012;  
14 Dupas et al., 2015c; Mellander et al., 2015). This modelling exercise also provides further  
15 support that SRP solubility was determined by the soil P Olsen content and could vary  
16 according to temperature and moisture conditions. The underlying processes have not been  
17 identified precisely in the Kervidy-Naizin catchment: independent laboratory experiments  
18 have shown that microbial cell lysis resulting from alternating dry and water saturated periods  
19 in the soil could be the cause of increased SRP mobility (Turner and Haygarth, 2001;  
20 Blackwell et al., 2009). This could explain the moisture dependence of SRP solubility in the  
21 model. Furthermore, net mineralisation of soil organic phosphorus could explain the  
22 temperature dependence of SRP solubility in the model. These two hypotheses may explain  
23 increased SRP solubility in soils in periods of dry and hot conditions and will be further  
24 explored by incubation experiment with soils from the Kervidy-Naizin catchments.

### 25 **4.2 Potential improvements to the model structure according to modelling** 26 **purpose**

27 The TNT2-P model was designed to test hypotheses about dominant processes and for this  
28 purpose, a parsimonious model structure was chosen to include only the processes which were  
29 to be tested. This parsimonious model structure might contain some conceptual  
30 misrepresentations due to oversimplification, and it might not include all the processes

1 necessary for the purpose of evaluating management scenarios. This section discusses  
2 whether the simplifications made are acceptable in the context of different catchment types,  
3 and to which conditions the model could be made more complex by including additional  
4 routines for the purpose of evaluating management scenarios.

5 From a conceptual point of view, the lack of cell-to-cell routing of SRP fluxes might result in  
6 erroneous results in some contexts. The fact that all the SRP emitted from each cell through  
7 overland flow and sub-surface flow reaches the stream on the same day is acceptable for the  
8 catchment studied because groundwater interception of shallow soil layers occurs in the  
9 riparian zone only, hence the signal of SRP mobilisation in these soils is generally transmitted  
10 to the stream (Dupas et al., 2015c). This simplification would not be acceptable in catchments  
11 where soil-groundwater interactions are taking place throughout the landscape, e.g. due to  
12 topographic depressions or poorly drained soils. In the latter type of catchment, transmission  
13 of the SRP mobilisation signal to the stream is more complex to comprehend (Haygarth et al.,  
14 2012), hence a more complex model structure would be required.

15 The reason for this simplification was that we lacked knowledge of SRP re-adsorption in  
16 downslope cells (or on suspended sediments in the stream network) and on the long-term fate  
17 of re-adsorbed SRP. For a more physically realistic representation of processes, it is likely  
18 that an explicit representation of flow velocities and pathways would be necessary, along with  
19 an explicit representation of several soil P pools. However, such an explicit representation of  
20 processes contradicts the idea of a parsimonious model, which was adopted here for the  
21 purpose of identifying dominant processes. In this respect, TNT2-P is an aggregative model  
22 rather than a fully distributed model although it is based on a fully distributed hydrological  
23 model (Beaujouan et al., 2002). The current spatial distribution allows finer representation of  
24 soil-groundwater interactions (i.e. the extend of the riparian wetland area) than semi-  
25 distributed models such as SWAT (Arnold et al., 1998), INCA-P (Wade et al., 2002) and  
26 HYPE (Lindstrom et al., 2010) but at higher computation cost. It would be interesting to test  
27 to which extent moving from an aggregative model with fully distributed information to a  
28 semi-distributed model would degrade the model performance and in the same time reduce  
29 computation cost. This could be achieved by grouping cells according to a hydrological  
30 similarity criterion like in Dynamic Topmodel (Beven and Freer, 2001b; Metcalfe et al.,  
31 2015) and do the same for similarity in soil P content.

1 If reducing the number of calculation units proved to reduce computation cost without  
2 degrading quality of prediction, it would be possible to include more parameters in the model,  
3 for example to simulate SRP re-absorption in downslope cells or include routines to simulate  
4 the evolution of soil P content under different management scenarios (Vadas et al., 2011;  
5 2012), and still perform a Monte-Carlo based analysis of uncertainty. The question of  
6 coupling or not such a soil P routine with the current TNT2-P model will depend on available  
7 data and on the length of available time series: studying the evolution of the soil P content  
8 requires at least a decade of soil observation data (Ringeval et al., 2014) and probably a  
9 longer period of stream data to account for the time delay for a perturbation in the catchment  
10 to become visible in the stream (Wall et al., 2013). Thus, the two years of daily stream SRP in  
11 the Kervidy-Naizin catchment are not enough to build a coupled soil-hydrology model with  
12 an elaborate soil P routine. Therefore, as things stand, it is more reasonable to generate new  
13 soil P Olsen maps with a separate model such as the APLE model (Vadas et al., 2012;  
14 Benskin et al., 2014) or the ‘soil P decline’ model used by Wall et al. (2013), and use these  
15 maps as input to TNT2-P.

16 Because the current model can simulate response to rainfall, soil moisture and temperature, it  
17 could be used to test the effect of climate scenarios on SRP transfer. In Western France, and  
18 more generally in Western Europe, the climate for the next few decades is expected to consist  
19 of hotter, drier summers and warmer, wetter winter (Jacob et al., 2007; Macleod et al., 2012;  
20 Salmon-Monviola et al., 2013) with increased frequency of high intensity rainfall events  
21 (Dequé 2007). In these conditions, SRP concentrations and load will seemingly increase  
22 compared to today’s climate as a result of both an increase in SRP solubility in soil due to  
23 higher temperature and more severe drought and an increase in transfer due to wetter winter  
24 and more frequent high intensity rainfall events. TNT2-P could be used to confirm and  
25 quantify the expected increase in SRP transfer from diffuse sources in future climate  
26 conditions.

### 27 **4.3 Improving information content in the data**

28 Despite relatively large uncertainty in the data used in this study, it was possible to build a  
29 parsimonious catchment model of SRP transfer for the purpose of testing hypotheses about  
30 dominant processes, namely the role of hydrology in controlling connectivity between soils  
31 and streams and the role of temperature and moisture conditions in controlling soil SRP  
32 solubilisation. However, the large uncertainties in the calibration data lead to large prediction

1 uncertainty. For example, the SRP load estimated by the behavioural models from 2013 to  
2 2015 ranged from 0.48 to 1.99 kg P ha<sup>-1</sup> yr<sup>-1</sup>; hence the width of the credibility interval was  
3 150% of the median (1 kg P ha<sup>-1</sup> yr<sup>-1</sup>). Similarly, the mean SRP concentration estimated by  
4 the behavioural models from 2013 to 2015 ranged from 0.014 to 0.044 mg l<sup>-1</sup>; hence the width  
5 of the credibility interval was 102% of the median (0.029 mg l<sup>-1</sup>). The large uncertainty in the  
6 calibration data, along with a lack of long-term information, also prevents including more  
7 detailed processes in the soil routine.

8 To reduce uncertainty in prediction and to build more complex models, several options exist  
9 to improve information content in the data. As stated by Jackson-Blake et al. (2015b), “the  
10 key to obtaining a realistic model simulation is ensuring that the natural variability in water  
11 chemistry is well represented by the monitoring data”. The monitoring strategy adopted in the  
12 Kervidy-Naizin catchment should theoretically enable to capture the natural variability in  
13 stream SRP concentration, because sampling took place during two contrasting water years,  
14 during different seasons and at a high frequency during 14 storm events. The analysis of  
15 uncertainty in the data shows that a large part of uncertainty in “observed” SRP concentration  
16 originates from sample storage, both unfiltered between the time of autosampling and manual  
17 filtration and between filtration and analysis. This is due to SRP being non-conservative.  
18 Thus, there is room for improvement in reducing storage time, without increasing further the  
19 monitoring frequency. In this respect, the primary interest of investing in high frequency  
20 bankside analysers would lie in their ability to analyse water samples immediately in addition  
21 to providing near continuous data. Because bankside analysers perform measurements in  
22 relatively homogeneous conditions, unlike the manual and autosampler data for which storage  
23 time of filtered and unfiltered samples vary, a finer quantification of uncertainty in the  
24 measurement data would be possible (e.g. Lloyd et al., 2015).

## 25 **5 Conclusion**

26 The TNT2-P model was capable of capturing daily variation of SRP loads, thus confirming  
27 the dominant processes identified in previous analyses of observation data in the Kervidy-  
28 Naizin catchment. The role of hydrology in controlling connectivity between soils and  
29 streams, and the role of soil Olsen P, soil moisture and temperature in controlling SRP  
30 solubility have been confirmed. The lack of any representation of the short-term effect of  
31 management practices did not seem to penalize the model’s performance. Their long-term  
32 effect on the soil Olsen P could be simulated with an independent model or through an

1 additional sub-model if a longer period of data was available to calibrate it. The modelling  
2 approach presented in this paper included an assessment of the information content in the  
3 data, and propagation of uncertainty in the model's prediction. The information content of the  
4 data was sufficient to explore dominant processes, but the relatively large uncertainty in SRP  
5 concentrations would seemingly limit the possibility for including more detailed processes  
6 into the model. Data from near continuous bankside analyser will probably allow calibrating  
7 more detailed models in the near future.

## 8 **References**

- 9 Alexander RB, Smith RA, Schwarz GE, Boyer EW, Nolan JV, Brakebill JW. Differences in  
10 phosphorus and nitrogen delivery to the gulf of Mexico from the Mississippi river basin.  
11 *Environmental Science & Technology* 2008; 42: 822-830.
- 12 Arnold JG, Srinivasan R, Muttiah RS, Williams JR. Large area hydrologic modeling and  
13 assessment - Part 1: Model development. *Journal of the American Water Resources*  
14 *Association* 1998; 34: 73-89.
- 15 Aubert AH, Gascuel-Oudoux C, Gruau G, Akkal N, Faucheux M, Fauvel Y, et al. Solute  
16 transport dynamics in small, shallow groundwater-dominated agricultural catchments:  
17 insights from a high-frequency, multisolute 10 yr-long monitoring study. *Hydrology and*  
18 *Earth System Sciences* 2013; 17: 1379-1391.
- 19 Beauchemin S, Simard RR. Soil phosphorus saturation degree: Review of some indices and  
20 their suitability for P management in Quebec, Canada. *Canadian Journal of Soil Science*  
21 1999; 79: 615-625.
- 22 Beaujouan V, Durand P, Ruiz L, Arousseau P, Cotteret G. A hydrological model dedicated  
23 to topography-based simulation of nitrogen transfer and transformation: rationale and  
24 application to the geomorphology-denitrification relationship. *Hydrological Processes* 2002;  
25 16: 493-507.
- 26 Benskin CMH, Roberts W. M, Wang Y, Haygarth PM. Review of the Annual Phosphorus  
27 Loss Estimator tool – a new model for estimating phosphorus losses at the field scale. *Soil*  
28 *Use and Management* 2014; 30: 337-341.
- 29 Beven K. A manifesto for the equifinality thesis. *Journal of Hydrology* 2006; 320: 18-36.
- 30 Beven K. *Environmental Modelling – An Uncertain Future?* Routledge: London 2009.

1 Beven K, Freer J. Equifinality, data assimilation, and uncertainty estimation in mechanistic  
2 modelling of complex environmental systems using the GLUE methodology. *Journal of*  
3 *Hydrology* 2001a; 249: 11-29.

4 Beven K, Freer J. A dynamic TOPMODEL. *Hydrological Processes* 2001b; 15: 1993-2011.

5 Beven K, Smith P. Concepts of Information Content and Likelihood in Parameter Calibration  
6 for Hydrological Simulation Models. *Journal of Hydrologic Engineering* 2015; 20.

7 Beven KJ. Distributed hydrological modelling: applications of the TOPMODEL concept,  
8 1997.

9 Blackwell MSA, Brookes PC, de la Fuente-Martinez N, Murray PJ, Snars KE, Williams JK,  
10 et al. Effects of soil drying and rate of re-wetting on concentrations and forms of phosphorus  
11 in leachate. *Biology and Fertility of Soils* 2009; 45: 635-643.

12 Blazkova S, Beven K. A limits of acceptability approach to model evaluation and uncertainty  
13 estimation in flood frequency estimation by continuous simulation: Skalka catchment, Czech  
14 Republic. *Water Resources Research* 2009; 45.

15 Bruneau P, Gascuel-Oudou C, Robin P, Merot P, Beven KJ. Sensitivity to space and time  
16 resolution of a hydrological model using digital elevation data. *Hydrological Processes* 1995;  
17 9: 69-82.

18 Carluer N. Vers une modélisation hydrologique adaptée à l'évaluation des pollutions diffuses:  
19 prise en compte du réseau anthropique. Application au bassin versant de Naizin (Morbihan).  
20 PhD thesis Université Pierre et Marie Curie 1998.

21 Carpenter SR, Caraco NF, Correll DL, Howarth RW, Sharpley AN, Smith VH. Nonpoint  
22 pollution of surface waters with phosphorus and nitrogen. *Ecological Applications* 1998; 8:  
23 559-568.

24 Coxon, G., Freer, J., Westerberg, I. K., Wagener, T., Woods, R., and Smith, P. J.: A novel  
25 framework for discharge uncertainty quantification applied to 500 UK gauging stations,  
26 *Water Resources Research*, 51, 5531-5546, 2015.

27 Curmi P, Durand P, Gascuel-Oudou C, Merot P, Walter C, Taha A. Hydromorphic soils,  
28 hydrology and water quality: spatial distribution and functional modelling at different scales.  
29 *Nutrient Cycling in Agroecosystems* 1998; 50: 127-142.

- 1 Dean S, Freer J, Beven K, Wade AJ, Butterfield D. Uncertainty assessment of a process-based  
2 integrated catchment model of phosphorus. *Stochastic Environmental Research and Risk*  
3 *Assessment* 2009; 23: 991-1010.
- 4 Deque M. Frequency of precipitation and temperature extremes over France in an  
5 anthropogenic scenario: Model results and statistical correction according to observed values.  
6 *Global and Planetary Change* 2007; 57: 16-26.
- 7 Dupas R, Delmas M, Dorioz JM, Garnier J, Moatar F, Gascuel-Oudou C. Assessing the  
8 impact of agricultural pressures on N and P loads and eutrophication risk. *Ecological*  
9 *Indicators* 2015a; 48: 396–407.
- 10 Dupas R, Gascuel-Oudou C, Gilliet N, Grimaldi C, Gruau G. Distinct export dynamics for  
11 dissolved and particulate phosphorus reveal independent transport mechanisms in an arable  
12 headwater catchment. *Hydrological Processes* 2015b.
- 13 Dupas R, Gruau G, Gu S, Humbert G, Jaffrezic A, Gascuel-Oudou C. Groundwater control of  
14 biogeochemical processes causing phosphorus release from riparian wetlands. *Water*  
15 *Research* 2015c.
- 16 Dupas R, Tavenard R, Fovet O, Gilliet N, Grimaldi C, Gascuel-Oudou C. Identifying seasonal  
17 patterns of phosphorus storm dynamics with Dynamic Time Warping. *Water Resources*  
18 *Research* 2015d.
- 19 Durand P, Moreau P, Salmon-Monviola J, Ruiz L, Vertes F, Gascuel-Oudou C. Modelling the  
20 interplay between nitrogen cycling processes and mitigation options in farming catchments.  
21 *Journal of Agricultural Science* 2015; 153: 959-974.
- 22 Franks SW, Gineste P, Beven KJ, Merot P. On constraining the predictions of a distributed  
23 model: the incorporation of fuzzy estimates of saturated areas into the calibration process,  
24 *Water Resources Research* 1998; 34: 787-797.
- 25 Grizzetti B, Bouraoui F, Aloe A. Changes of nitrogen and phosphorus loads to European seas.  
26 *Global Change Biology* 2012; 18: 769-782.
- 27 Hahn C, Prasuhn V, Stamm C, Lazzarotto P, Evangelou MWH, Schulin R. Prediction of  
28 dissolved reactive phosphorus losses from small agricultural catchments: calibration and  
29 validation of a parsimonious model. *Hydrology and Earth System Sciences* 2013; 17: 3679-  
30 3693.

1 Hahn C, Prasuhn V, Stamm C, Schulin R. Phosphorus losses in runoff from manured  
2 grassland of different soil P status at two rainfall intensities. *Agriculture Ecosystems &*  
3 *Environment* 2012; 153: 65-74.

4 Haygarth PM, Ashby CD, Jarvis SC. Short-term changes in the molybdate reactive  
5 phosphorus of stored soil waters. *Journal of Environmental Quality* 1995; 24: 1133-1140.

6 Haygarth PM, Hepworth L, Jarvis SC. Forms of phosphorus transfer in hydrological pathways  
7 from soil under grazed grassland. *European Journal of Soil Science* 1998; 49: 65-72.

8 Haygarth PM, Page TJC, Beven KJ, Freer J, Joynes A, Butler P, et al. Scaling up the  
9 phosphorus signal from soil hillslopes to headwater catchments. *Freshwater Biology* 2012;  
10 57: 7-25.

11 Heathwaite AL, Dils RM. Characterising phosphorus loss in surface and subsurface  
12 hydrological pathways. *Science of the Total Environment* 2000; 251: 523-538.

13 Heckrath G, Brookes PC, Poulton PR, Goulding KWT. Phosphorus leaching from soils  
14 containing different phosphorus concentrations in the broadbalk experiment. *Journal of*  
15 *Environmental Quality* 1995; 24: 904-910.

16 Hornberger GM, Spear RC. An approach to the preliminary analysis of environmental  
17 systems. *J. Environmental Management* 1981; 12: 7-18.

18 Jackson-Blake LA, Dunn SM, Helliwell RC, Skeffington RA, Stutter MI, Wade AJ. How well  
19 can we model stream phosphorus concentrations in agricultural catchments? *Environmental*  
20 *Modelling & Software* 2015a; 64: 31-46.

21 Jackson-Blake LA, Starrfelt J. Do higher data frequency and Bayesian auto-calibration lead to  
22 better model calibration? Insights from an application of INCA-P, a process-based river  
23 phosphorus model. *Journal of Hydrology* 2015b; 527: 641-655.

24 Jacob D, Barring L, Christensen OB, Christensen JH, de Castro M, Deque M, et al. An inter-  
25 comparison of regional climate models for Europe: model performance in present-day  
26 climate. *Climatic Change* 2007; 81: 31-52.

27 Jarvie HP, Withers PJA, Neal C. Review of robust measurement of phosphorus in river water:  
28 sampling, storage, fractionation and sensitivity. *Hydrology and Earth System Sciences* 2002;  
29 6: 113-131.



1 Jordan P, Melland AR, Mellander PE, Shortle G, Wall D. The seasonality of phosphorus  
2 transfers from land to water: implications for trophic impacts and policy evaluation. *Sci Total*  
3 *Environ* 2012; 434: 101-9.

4 Kirchner JW. Getting the right answers for the right reasons: Linking measurements,  
5 analyses, and models to advance the science of hydrology. *Water Resources Research* 2006;  
6 42.

7 Krueger T, Quinton JN, Freer J, Macleod CJA, Bilotta GS, Brazier RE, Hawkins JMB,  
8 Haygarth PM. Comparing empirical models for sediment and phosphorus transfer from soils  
9 to water at field and catchment scale under data uncertainty. *European Journal of Soil Science*  
10 2012; 63(2): 211–223.

11 Humbert G, Jaffrezic A, Fovet O, Gruau G, Durand P. Dry-season length and runoff control  
12 annual variability in stream DOC dynamics in a small, shallow groundwater-dominated  
13 agricultural watershed. *Water Resources Research* 2015.

14 Lazzarotto P, Stamm C, Prasuhn V, Flühler H. A parsimonious soil-type based rainfall-runoff  
15 model simultaneously tested in four small agricultural catchments. *Journal of Hydrology*  
16 2006; 321: 21-38.

17 Lindstrom G, Pers C, Rosberg J, Stromqvist J, Arheimer B. Development and testing of the  
18 HYPE (Hydrological Predictions for the Environment) water quality model for different  
19 spatial scales. *Hydrology Research* 2010; 41: 295-319.

20 Lloyd CEM, Freer JE, Johnes PJ, Coxon G, Collins AL. Discharge and nutrient uncertainty:  
21 implications for nutrient flux estimation in small streams. *Hydrological processes* 2015.

22 Macleod CJA, Falloon PD, Evans R, Haygarth PM. The effects of climate change on the  
23 mobilization of diffuse substances from agricultural systems. In: Sparks DL, editor. *Advances*  
24 *in Agronomy*, Vol 115. 115, 2012, pp. 41-77.

25 Maguire RO, Sims JT. Soil testing to predict phosphorus leaching. *Journal of Environmental*  
26 *Quality* 2002; 31: 1601-1609.

27 Matos-Moreira M, Lemercier B, Michot D, Dupas R, Gascuel-Odoux C. Using agricultural  
28 practices information for multiscale environmental assessment of phosphorus risk.  
29 *Geophysical Research Abstracts* 2015; 17.

1 McDowell R, Sharpley A, Withers P. Indicator to predict the movement of phosphorus from  
2 soil to subsurface flow. *Environmental Science & Technology* 2002; 36: 1505-1509.

3 McMillan, H., Krueger, T., and Freer, J.: Benchmarking observational uncertainties for  
4 hydrology: rainfall, river discharge and water quality, *Hydrological Processes*, 26, 4078-4111,  
5 2012.

6 Mellander PE, Jordan P, Shore M, Melland AR, Shortle G. Flow paths and phosphorus  
7 transfer pathways in two agricultural streams with contrasting flow controls. *Hydrological*  
8 *Processes* 2015.

9 Metcalfe P, Beven BJ, and Freer J. Dynamic Topmodel: a new implementation in R and its  
10 sensitivity to time and space steps. *Environmental Modelling and Software* 2015; 72: 155-  
11 172.

12 Molenat J, Gascuel-Oudou C, Ruiz L, Gruau G. Role of water table dynamics on stream  
13 nitrate export and concentration. in agricultural headwater catchment (France). *Journal of*  
14 *Hydrology* 2008; 348: 363-378.

15 Moore MT, Locke MA. Effect of Storage Method and Associated Holding Time on Nitrogen  
16 and Phosphorus Concentrations in Surface Water Samples. *Bulletin of Environmental*  
17 *Contamination and Toxicology* 2013; 91: 493-498.

18 Moreau P, Ruiz L, Mabon F, Raimbault T, Durand P, Delaby L, et al. Reconciling technical,  
19 economic and environmental efficiency of farming systems in vulnerable areas. *Agriculture*  
20 *Ecosystems & Environment* 2012; 147: 89-99.

21 Moreau P, Viaud V, Parnaudeau V, Salmon-Monviola J, Durand P. An approach for global  
22 sensitivity analysis of a complex environmental model to spatial inputs and parameters: A  
23 case study of an agro-hydrological model. *Environmental Modelling & Software* 2013; 47:  
24 74-87.

25 Moriasi DN, Arnold JG, Van Liew MW, Bingner RL, Harmel RD, Veith TL. Model  
26 evaluation guidelines for systematic quantification of accuracy in watershed simulations.  
27 *Transactions of the Asabe* 2007; 50: 885-900.

28 Olsen SR, Cole CV, Watanbe FS, Dean LA. Estimation of available phosphorus in soils by  
29 extraction with sodium bicarbonate 1954.. *Circ. 939. USDA, Washington, DC.*

1 Outram FN, Lloyd CEM, Jonczyk J, Benskin CMH, Grant F, Perks MT, et al. High-frequency  
2 monitoring of nitrogen and phosphorus response in three rural catchments to the end of the  
3 2011-2012 drought in England. *Hydrology and Earth System Sciences* 2014; 18: 3429-3448.

4 Page T, Haygarth PM, Beven KJ, Joynes A, Butler T, Keeler C, et al. Spatial variability of  
5 soil phosphorus in relation to the topographic index and critical source areas: Sampling for  
6 assessing risk to water quality. *Journal of Environmental Quality* 2005; 34: 2263-2277.

7 Perks MT, Owen GJ, Benskin CMH, Jonczyk J, Deasy C, Burke S, et al. Dominant  
8 mechanisms for the delivery of fine sediment and phosphorus to fluvial networks draining  
9 grassland dominated headwater catchments. *Science of the Total Environment* 2015; 523:  
10 178-190.

11 Quinlan, J.R. Learning with continuous classes. *Proceedings of the 5th Australian Joint*  
12 *Conference On Artificial Intelligence* 1992, 343-348.

13 Rode M, Suhr U. Uncertainties in selected river water quality data. *Hydrology and Earth*  
14 *System Sciences* 2007; 11(2): 863-874.

15 Ringeval B, Nowak B, Nesme T, Delmas M, Pellerin S. Contribution of anthropogenic  
16 phosphorus to agricultural soil fertility and food production. *Global Biogeochemical Cycles*  
17 2014; 28: 743-756.

18 Salmon-Monviola J, Moreau P, Benhamou C, Durand P, Merot P, Oehler F, et al. Effect of  
19 climate change and increased atmospheric CO<sub>2</sub> on hydrological and nitrogen cycling in an  
20 intensive agricultural headwater catchment in western France. *Climatic Change* 2013; 120:  
21 433-447.

22 Schindler DW, Hecky RE, Findlay DL, Stainton MP, Parker BR, Paterson MJ, et al.  
23 Eutrophication of lakes cannot be controlled by reducing nitrogen input: Results of a 37-year  
24 whole-ecosystem experiment. *Proceedings of the National Academy of Sciences of the United*  
25 *States of America* 2008; 105: 11254-11258.

26 Schoumans OF, Chardon WJ. Phosphate saturation degree and accumulation of phosphate in  
27 various soil types in The Netherlands. *Geoderma* 2015; 237: 325-335.

28 Serrano T, Dupas R, Upegui E, Buscail C, Grimaldi C, Viel J-F. Geographical modeling of  
29 exposure risk to cyanobacteria for epidemiological purposes. *Environment International* 2015;  
30 81: 18-25.

- 1 Sharpley AN, Kleinman PJ, Heathwaite AL, Gburek WJ, Folmar GJ, Schmidt JP. Phosphorus  
2 loss from an agricultural watershed as a function of storm size. *J Environ Qual* 2008; 37: 362-  
3 8.
- 4 Siwek J, Siwek JP, Zelazny M. Environmental and land use factors affecting phosphate  
5 hysteresis patterns of stream water during flood events (Carpathian Foothills, Poland).  
6 *Hydrological Processes* 2013; 27: 3674-3684.
- 7 Turner BL, Haygarth PM. Biogeochemistry - Phosphorus solubilization in rewetted soils.  
8 *Nature* 2001; 411: 258-258.
- 9 Vadas PA, Joern BC, Moore PA. Simulating soil phosphorus dynamics for a phosphorus loss  
10 quantification tool. *J Environ Qual* 2012; 41: 1750-7.
- 11 Vadas PA, Jokela WE, Franklin DH, Endale DM. The Effect of Rain and Runoff When  
12 Assessing Timing of Manure Application and Dissolved Phosphorus Loss in Runoff1.  
13 *JAWRA Journal of the American Water Resources Association* 2011; 47: 877-886.
- 14 Wade AJ, Whitehead PG, Butterfield D. The Integrated Catchments model of Phosphorus  
15 dynamics (INCA-P), a new approach for multiple source assessment in heterogeneous river  
16 systems: model structure and equations. *Hydrology and Earth System Sciences* 2002; 6: 583-  
17 606.
- 18 Wall DP, Jordan P, Melland AR, Mellander PE, Mechan S, Shortle G. Forecasting the decline  
19 of excess soil phosphorus in agricultural catchments. *Soil Use and Management* 2013; 29:  
20 147-154.
- 21 Whitehead PG, Hornberger GE. Modelling algal behaviour in the River Thames, *Water*  
22 *Research* 1984; 18: 945-953.
- 23 Wade AJ, Whitehead PG, Hornberger GE, Snook D. On Modelling the flow controls on  
24 macrophytes and epiphyte dynamics in a lowland permeable catchment: the River Kennet,  
25 southern England. *Sci Tot Environ* 2002b: 282-283: 395-417.
- 26 Whitehead P, Young P. Water-quality in river systems – Monte-Carlo analysis. *Water*  
27 *Resources Research* 1979; 15: 451-459.

## 28 **Acknowledgements**

- 1 This work was funded by the “Agence de l’Eau Loire Bretagne” via the “Trans-P project”.
- 2 Long-term monitoring in the Kervidy-Naizin catchment is supported by “ORE AgrHyS”.
- 3 Data of “ORE AgrHyS” can be downloaded from [http://www6.inra.fr/ore\\_agrhys/Donnees](http://www6.inra.fr/ore_agrhys/Donnees).

4

5

1 Table 1: Initial parameter ranges in the hydrological and soil phosphorus sub models.

	Abbreviation	Unit	Hydrological (H), Phosphorus model (P)	Range poorly drained soils (min-max)	Range well drained soils (min-max)
Lateral transmissivity at saturation	T	$m^2 d^{-1}$	H	4-8	-> x1.5
Exponential decay rate of hydraulic conductivity with depth	m	$m^2 d^{-1}$	H	0.02-0.2	0.02-0.2
Soil depth	ho	m	H	0.3-0.8	-> x1
Drainage porosity of soil	po	$cm^3 cm^{-3}$	H	0.1-0.4	-> x1
Regolith layer thickness	h1	m	H	5-10	-> x4
Exponent for evaporation limit	A	-	H	8 (fixed)	-> x1
kRC parameter for capillary rise	kRC	-	H	0.001 (fixed)	-> x1
n parameter for capillarity rise	N	-	H	2.5 (fixed)	-> x1
Drainage porosity of regolith layer	p1	$cm^3 cm^{-3}$	H	0.01-0.05	-> x1
Background P release coefficient for subsurface flow	Coef <sub>SRP</sub> overland	-	P	0-0.015	-> x1
Background P release coefficient for overland flow	Coef <sub>SRP</sub> sub-surface	-	P	0-0.25	-> x1
Temperature coefficient 1	T1	-	P	5-10	-> x1
Temperature coefficient 2	T2	-	P	2-10	-> x1

<b>Soil moisture coefficient</b>	S1	-	P	0-2	-> x1
<b>SRP concentration in deep flow</b>	SRP_deep	mg l <sup>-1</sup>	P	0-0.007	-> x1

1

2 Table 2: Starting and ending dates of periods studied

<b>Name</b>	<b>Starting date</b>	<b>Ending date</b>
<b>Autumn 2013</b>	01 October 2013	31 December 2013
<b>Winter 2014</b>	01 January 2014	31 March 2014
<b>Spring 2014</b>	01 April 2014	31 July 2014
<b>Autumn 2014</b>	01 October 2014	31 December 2014
<b>Winter 2015</b>	01 January 2015	31 March 2015
<b>Spring 2015</b>	01 April 2015	31 July 2015

3

4

1 Table 3: Sensitivity analysis of the model to 18 model parameters (insignificant ., important \*,  
 2 critical \*\*\*). Parameters significations are detailed in Table 1.

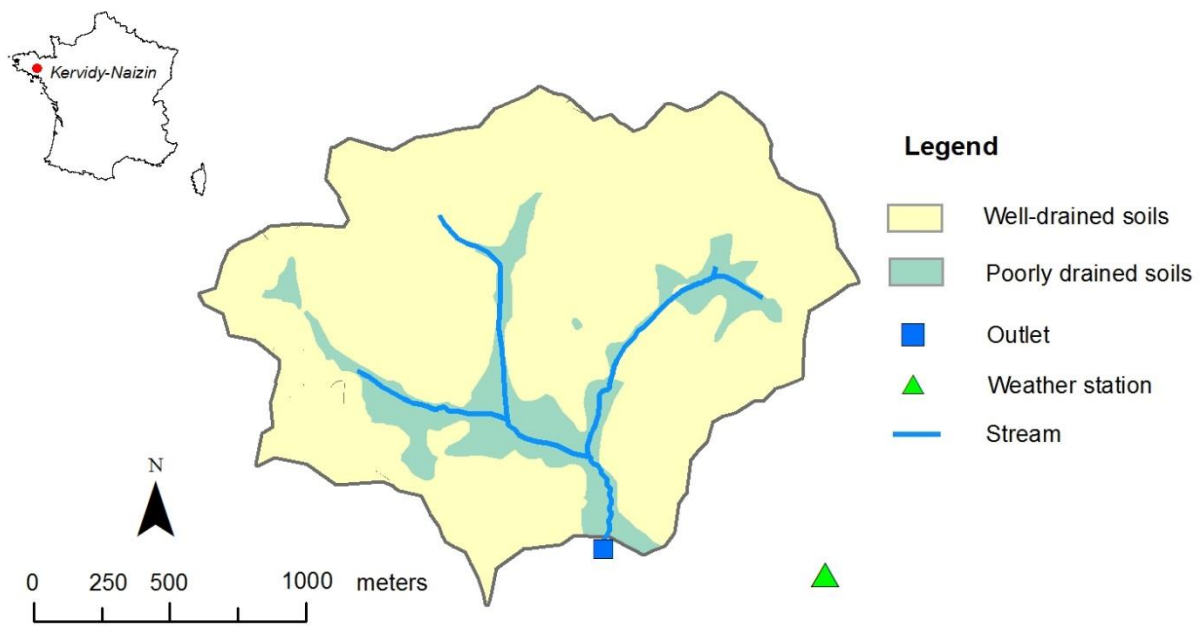
3

	discharge	baseflow SRP load	storm SRP load
<b>T (poorly drained soils)</b>	.	***	***
<b>m (poorly drained soils)</b>	***	***	***
<b>ho (poorly drained soils)</b>	***	***	.
<b>po (poorly drained soils)</b>	***	***	***
<b>h1 (poorly drained soils)</b>	***	***	.
<b>p1 (poorly drained soils)</b>	***	***	***
<b>T (well drained soils)</b>	.	***	***
<b>m (well drained soils)</b>	***	***	***
<b>ho (well drained soils)</b>	***	***	.
<b>po (well drained soils)</b>	***	***	***
<b>h1 (well drained soils)</b>	***	***	.
<b>p1 (well drained soils)</b>	***	***	***
<b>Coef_sub-surface</b>	.	***	.
<b>Coef_overland</b>	.	***	***
<b>SRP_deep</b>	.	.	.
<b>S1</b>	.	***	***
<b>T1</b>	.	***	***
<b>T2</b>	.	***	***

4

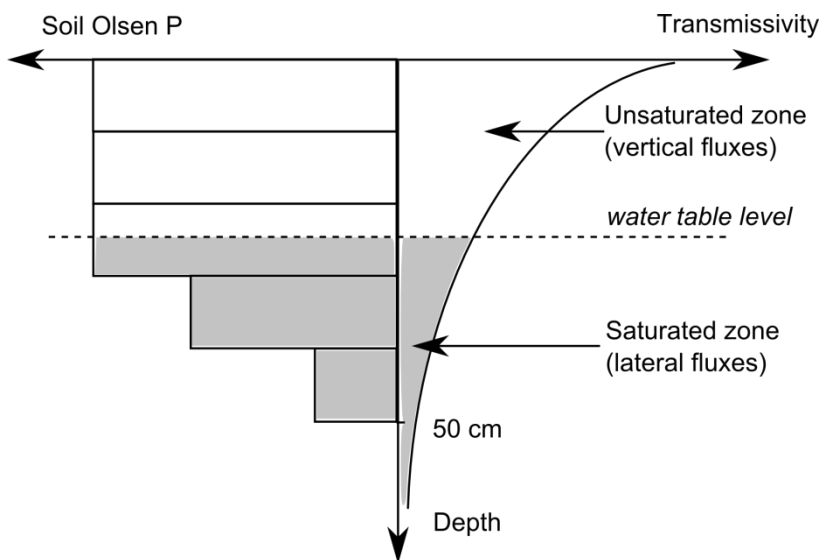
5





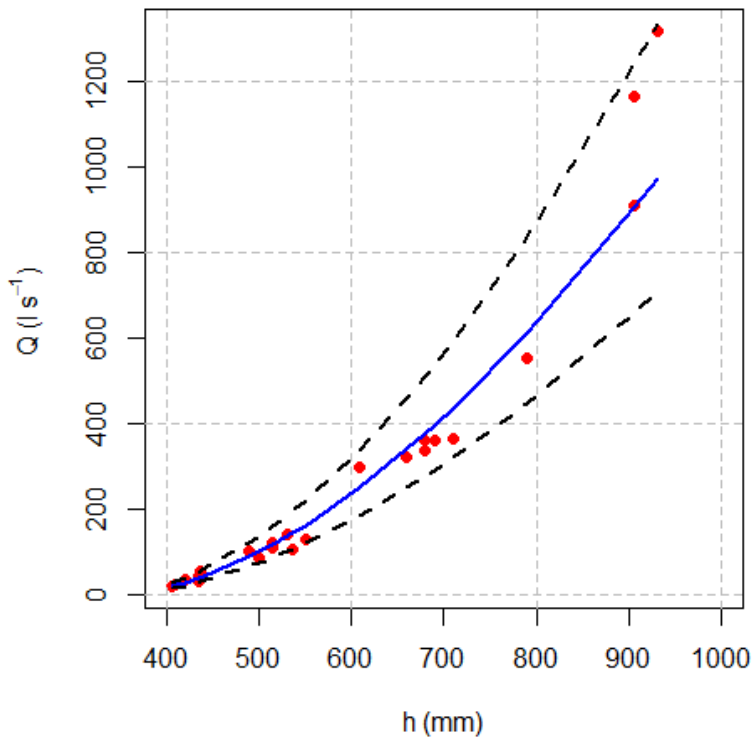
1

2 Fig. 1. Soil drainage classes in the Kervidy-Naizin catchment, Curmi et al. (1998)



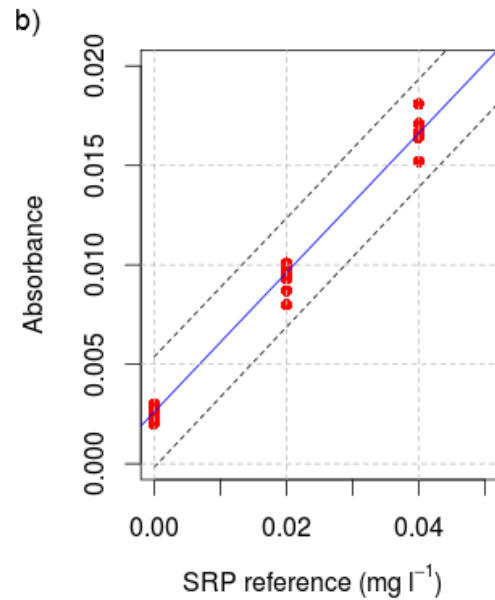
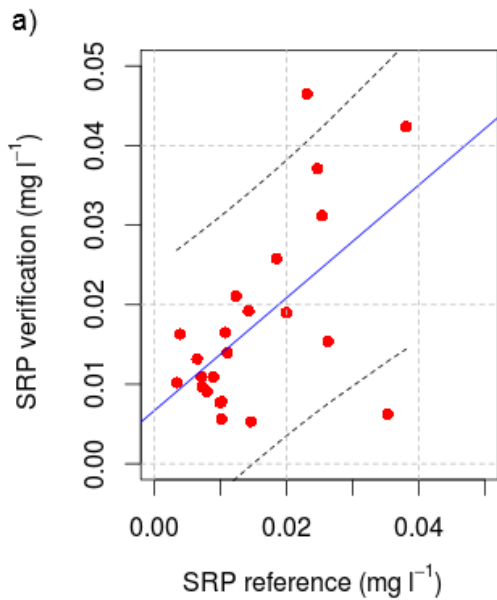
3

4 Fig. 2. Description of soil hydraulic properties and phosphorus content with depth



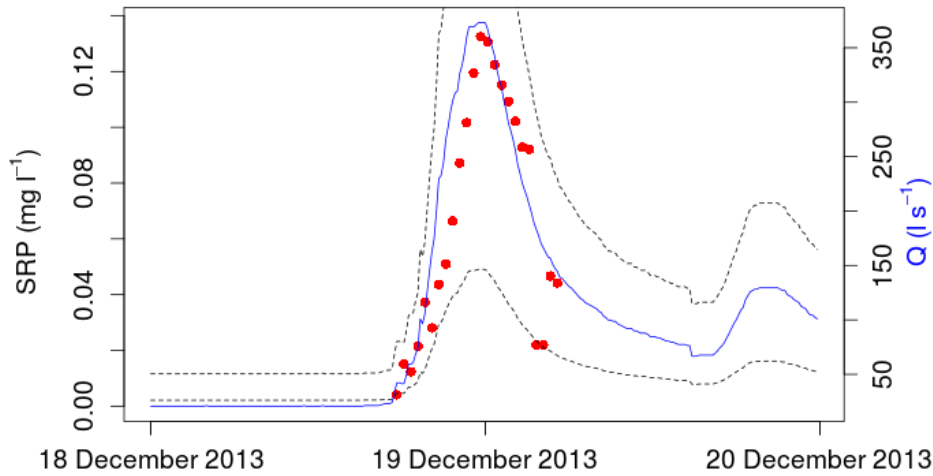
1

2 Fig. 3 : Rating curve in Kervidy-Naizin; acceptability bounds derived from 90% prediction  
 3 interval (blue line: fitting regression; black dots: 90% prediction interval). Red dots represent  
 4 the original discharge measurements used to calibrate the stage-discharge rating curve  
 5 (Carluer, 1998).

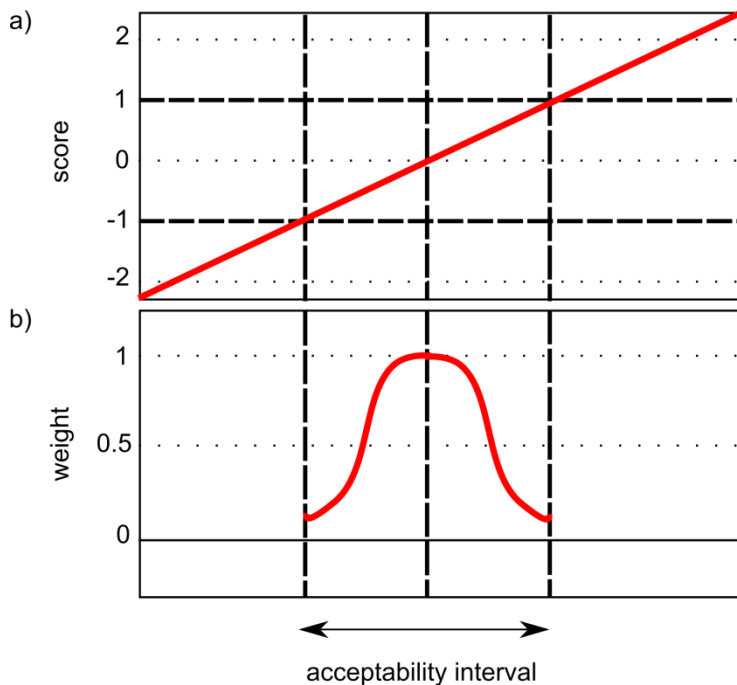


6

1 Fig. 4: a) linear regression model linking the reference data and a verification dataset; b)  
 2 measurement error as estimated from a repeatability test performed by the lab in charge of  
 3 producing reference data (blue line: fitting regression; black dots: 90% prediction interval).  
 4

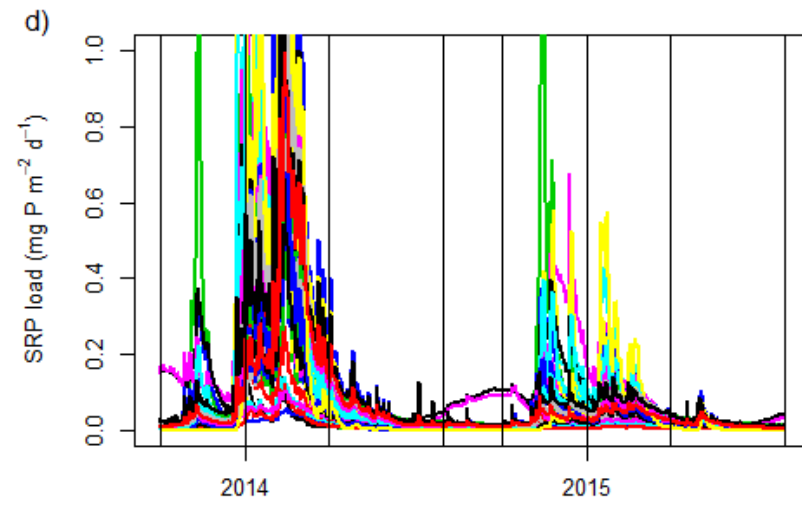
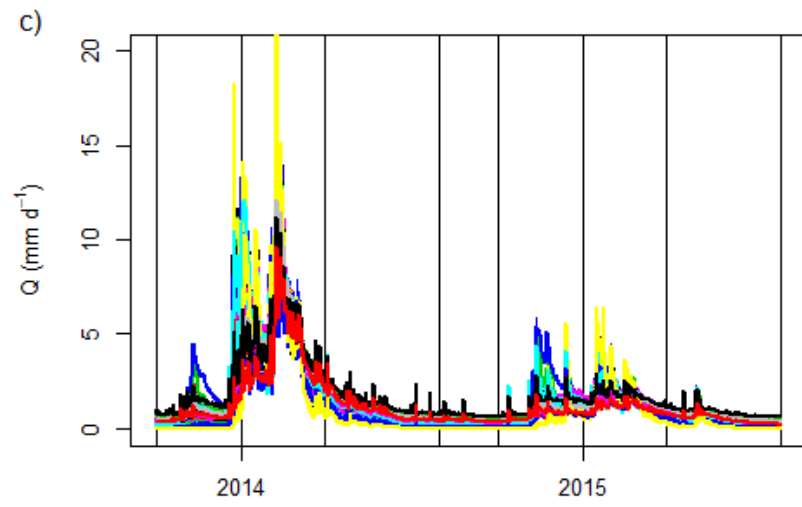
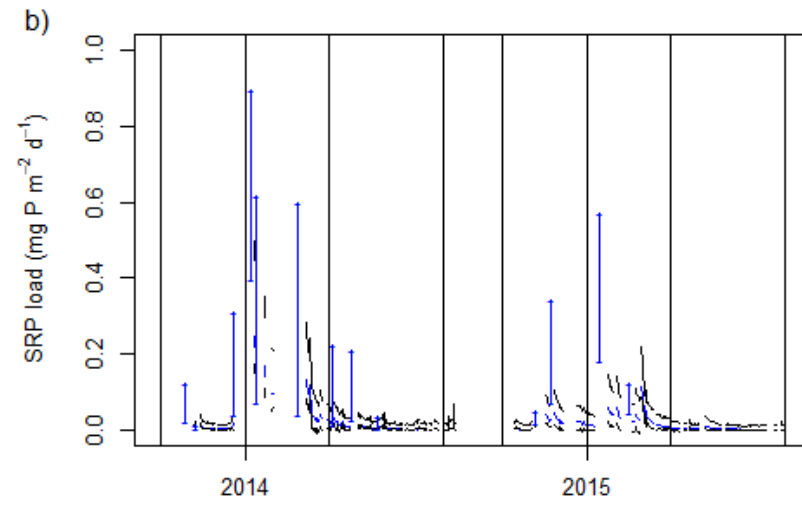
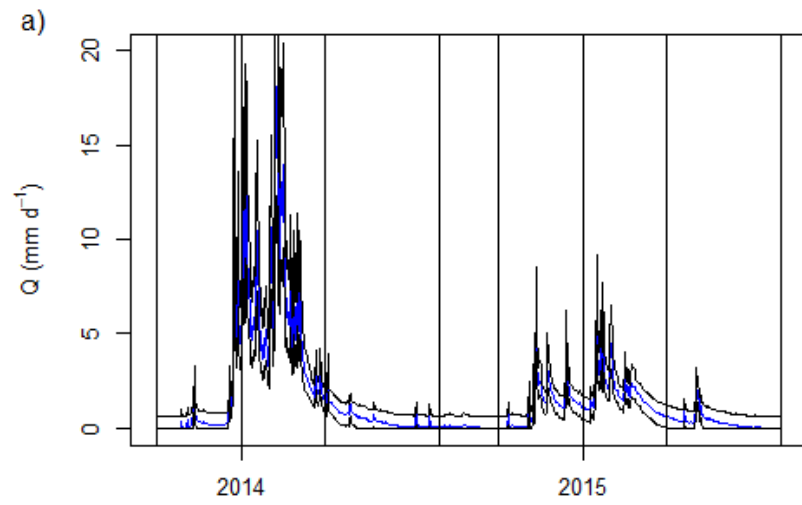


5  
 6 Fig. 5: Example of an empirical concentration – discharge model; acceptability bounds  
 7 derived from 90% prediction interval. Red circles represent the SRP measurements.  
 8



9  
 10 Fig. 6 : a) normalized scores; b) weighting function

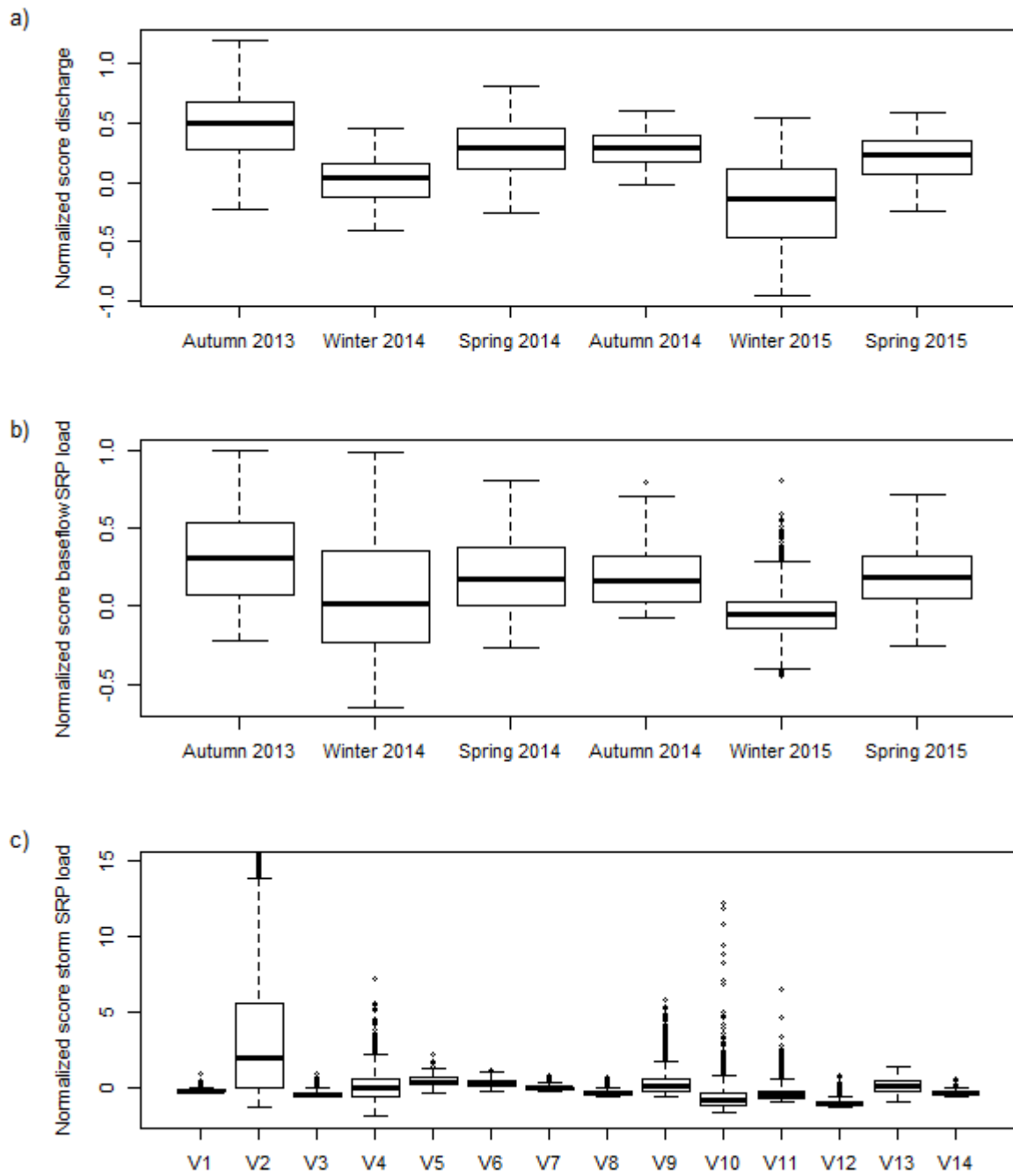
1



2

1 Fig. 7: Acceptability limits for daily discharge (a) and SRP load (b). Blue lines represent best estimates; black lines represent the acceptability  
2 limits. Storm loads acceptability limits are represented by vertical blue lines. And example of 50 model runs simulating discharge (c) and  
3 daily load (d). Black vertical lines represent the starting and ending dates for each season (table 2).

1

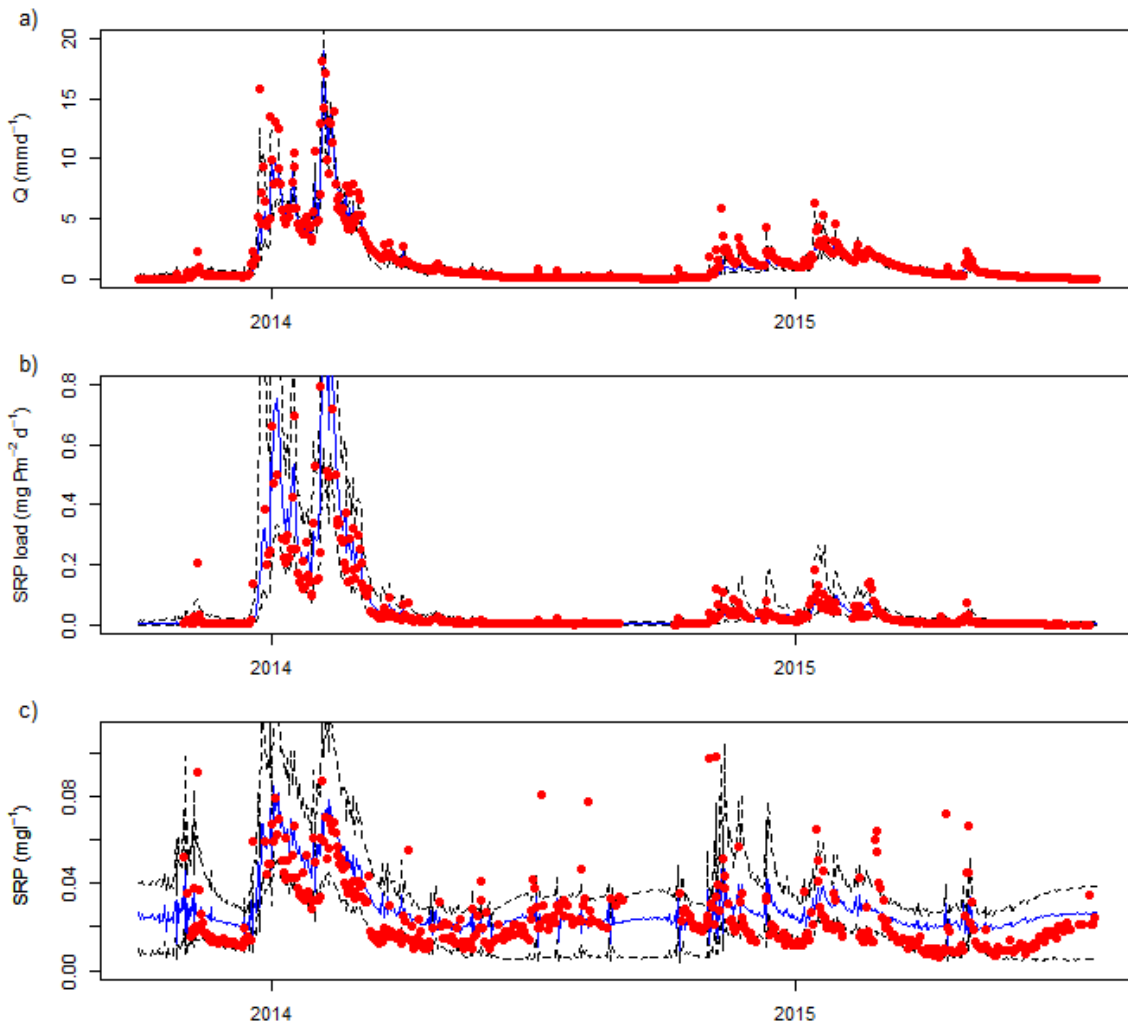


2

3 Fig. 8: Normalized score for daily discharge (a), baseflow SRP load (b) and storm SRP load

4 (c).

5



1

2 Fig. 9: Median and 95% credibility interval for daily discharge (a), SRP load (b) and SRP  
 3 concentration (c). Red circles represent observational data.

4